LBL-34092
UC-401
Preprint

Lawrence Berkeley Laboratory
UNIVERSITY OF CALIFORNIA

CHEMICAL SCIENCES DIVISION

Submitted to Journal of Chemical Physics

The Near Ultraviolet Photodissociation Dynamics of Azomethane

S.W. North, C.A. Longfellow and Y.T. Lee

May 1993

REFERENCE COPY
Does Not
Circulate
Bldg. 50 Library.
LBL-34092
Copy 1

Prepared for the U.S. Department of Energy under Contract Number DE-AC03-76SF00098

DISCLAIMER

This document was prepared as an account of work sponsored by the United States Government. While this document is believed to contain correct information, neither the United States Government nor any agency thereof, nor the Regents of the University of California, nor any of their employees, makes any warranty, express or implied, or assumes any legal responsibility for the accuracy, completeness, or usefulness of any information, apparatus, product, or process disclosed, or represents that its use would not infringe privately owned rights. Reference herein to any specific commercial product, process, or service by its trade name, trademark, manufacturer, or otherwise, does not necessarily constitute or imply its endorsement, recommendation, or favoring by the United States Government or any agency thereof, or the Regents of the University of California. The views and opinions of authors expressed herein do not necessarily state or reflect those of the United States Government or any agency thereof or the Regents of the University of California.

LBL-34092
UC-401

THE NEAR ULTRAVIOLET PHOTODISSOCIATION DYNAMICS OF AZOMETHANE

Simon W. North, Cheryl A. Longfellow and Yuan T. Lee

Chemical Sciences Division
Lawrence Berkeley Laboratory,

and

Department of Chemistry
University of California
Berkeley, California 94720, USA

May 1993

This work was supported by the Director, Office of Energy Research, Office of Basic Energy Sciences, Chemical Sciences Division, of the U.S. Department of Energy under Contract No. DE-AC03-76SF00098.

The Near Ultraviolet Photodissociation Dynamics of Azomethane

Simon W. North, Cheryl A. Longfellow, Yuan T. Lee

Chemical Sciences Division, Lawrence Berkeley Laboratory, and Department of Chemistry, University of California, Berkeley, California, 94720, USA

Abstract

The photodissociation of azomethane following absorption of a single 351 nm photon was studied using the method of molecular beam photofragment translational spectroscopy. The dissociation was observed to proceed via cleavage of both C-N bonds to yield N_2 and two methyl radicals. The measured time-of-flight spectra show evidence that the two methyl radicals possess unequal velocities in the azomethane center-of-mass suggesting that the dissociation is not symmetric. The angles between the asymptotic center-of-mass velocities for all three fragments are strongly correlated implying that the methyldiazenyl radical (CH_3N_2) intermediate decomposes within a fraction of its rotational period. We conclude, therefore, that the dissociation is *concerted* not stepwise as was inferred from recent time-resolved experiments. The overall translational energy distributions for all the photofragments in the azomethane center-of-mass reveal that an average of 59.6% of the total available energy appears as translation. A possible mechanism, consistent with the experimental findings, will be proposed and discussed.

I. Introduction

Azoalkanes are an interesting class of organic compounds whose photochemistry has been extensively studied for many years.[1] The characteristic near ultraviolet diffuse absorption band has been attributed to an n->π^* transition.[2] This electric dipole forbidden transition corresponds to a singlet (S_0) to singlet (S_1) excitation. Although this results in *cis-trans* isomerization in *condensed phases,* the dominant fate of acyclic azoalkanes in the *gas phase* is dissociation into alkyl radicals and nitrogen.[3] The most palatable aspect of symmetric azoalkanes as radical precursors is that N_2 is the sole byproduct. The photolytic decomposition of azoalkanes has therefore proven to be a viable source of alkyl radicals for kinetic[4], spectroscopic[5], and dynamics[6] measurements.

The simplicity of azomethane makes it a potential *benchmark* in both the theoretical understanding and the experimental investigation of azoalkane photodissociation dynamics. *Ab initio* results predict that the first excited singlet is labile about the N-N bond and that crossing to the ground state surface may occur at a dihedral angle of 90°.[7] Whether or not internal conversion (IC) occurs efficiently in the *gas phase* will determine if photodissociation proceeds via an identical mechanism to thermolysis. If the dissociation does not occur on the ground state potential energy surface then azomethane could dissociate from either the energetically accessible S_1 or first excited triplet state.[8] Rates of intersystem crossing (ISC) for azoalkanes have been predicted to range from rapid[9] to slow[10]. Although many experimental techniques[1,11] have been used to assess the participation of the triplet state in azoalkane photochemistry the results are often contradictory. Despite the vast quantity of research on azoalkane photochemistry, the electronic state(s) involved and the mechanism of dissociation remain the subject of much speculation.

If sufficient energy is deposited in a molecule to insure the eventual cleavage of two bonds, the sequence of events that lead to the multiple bond rupture is of fundamental mechanistic importance. Often in photodissociation studies of halocarbons involving secondary processes the initial step is direct and results in a highly vibrationally excited photofragment. The rate of decomposition of the photoproduct is then a function of its internal energy. Those possessing vibrational energy above the barrier to dissociation undergo secondary fragmentation while those with insufficient vibrational energy persist. Such a dissociation is termed *stepwise*. If the cleavages of both bonds are strongly coupled, occurring in a "single kinetic step"[12], then the dissociation pathway is considered a concerted process. Recently, a detailed study of acetone dissociation following excitation to the ^{1}(n,3s) Rydberg state, yielded nascent product state distributions and CH_3 translational energy distributions that suggested a non-synchronous concerted mechanism.[13,14]

Recent work by Weisman *et. al.* [15-17] using time-resolved coherent anti-stokes Raman spectroscopy (CARS) yielded the first direct information on the detailed dynamics of azomethane photodissociation. The experiment endeavored to answer the salient question of whether or not the dissociation proceeds via a concerted or a stepwise mechanism. Although there is recent consensus on gas phase thermolysis proceeding by initial single bond scission[18], there had been no experimental evidence on the lifetime of the CH_3N_2 intermediate. In the work of Weisman *et. al.*, the dissociation following excitation to the S_1 state, was concluded to be *stepwise* (1a-b).[17]

$$CH_3N_2CH_3 \xrightarrow{n \rightarrow \pi^*} CH_3 + [CH_3N_2]^{\ddagger} \qquad (1a)$$

$$[CH_3N_2]^{\ddagger} \longrightarrow CH_3 + N_2 \qquad (1b)$$

Under *collisional* conditions different appearance kinetics were observed for two quantum states of CH_3. Each quantum state was then attributed to a separate dissociation step. The 1st step was shown to be instantaneous within the ~1 ns experimental time resolution and the onset of the second methyl at 5.3 ± 1 ns provided evidence of a finite methyldiazenyl radical lifetime.

The distinction between concerted and stepwise mechanisms rests in the lifetime and inherent stability of the CH_3N_2 intermediate. The decomposition of methyldiazenyl radical (CH_3N_2) is postulated to be exothermic with an exit barrier ranging from as low as ~1.2 kcal/mole[19] to as high as 6.3-17.4 kcal/mole.[20,21] The existence of a barrier for methyldiazenyl decomposition implies that the lifetime of this fragment, and hence the overall dissociation mechanism, will be strongly dependent on both the height of the exit barrier and the internal energy of the nascent CH_3N_2. Assuming that the barrier is close to the most recently reported value of 1 kcal/mole, the 5.3 ns CH_3N_2 lifetime determined previously[16] appears anomalously long. The role of collisional deactivation, however, was considered to be important.[22] Under the *collisionless* conditions of a molecular beam experiment, elucidation of the initial dissociation dynamics that are a result of intrinsic properties of azomethane is feasible, as is investigation of the dissociation of the methyldiazenyl radical without the complications of secondary collisions.

This paper describes the recent investigation of azomethane photodissociation at 351 nm using photofragment translation spectroscopy. The translational energy and angular distributions for the photofragments determined in this study provide insight into both the partitioning of the

available energy in the dissociation and *temporal* information on the time delay between CH_3 eliminations.

II. Experimental

These measurements were performed on a molecular beam apparatus with a fixed source and a rotatable detector that has been described previously.[23] The machine has been modified to allow study of molecular photodissociation (Figure 1). A pulsed valve[24] (1.0 mm nozzle) utilizing a Physik-Instrumente piezocrystal was operated at 50 Hz. Helium was bubbled through azomethane held at -55°C resulting in a ~15% mixture with a total pressure behind the nozzle of 350 torr. A time-of-flight method was used with a spinning slotted wheel to measure the velocity and velocity spread of the molecular beam. An appropriate time delay between the wheel and the pulsed valve insured accurate sampling of the irradiated region of the pulse. The beam velocity was 10.4×10^4 cm/sec with a full width at half maximum (FWHM) spread of 20%. Although narrower spreads in beam velocity could be achieved in the dense part of the beam pulse the formation of dimers necessitated using the earlier, "warmer", leading edge.[25]

The resulting pulsed beam was collimated with two skimmers to a FWHM angular divergence of less than 3° and crossed at 90° with the output of a Lambda Physik EMG 202 MSC excimer laser operating at the XeF transition. The laser was run at 50 mJ/pulse and focused to a 2x4 mm spot. The laser was typically delayed 30 μsec from the onset of the molecular beam pulse allowing time for the molecules to move from the nozzle to the interaction region. The neutral photofragments recoiled 20.8 cm where they were detected by an electron bombardment ionizer quadrupole mass spectrometer. Data was collected by a computer interfaced multi-channel scaler trigged from the laser pulse.

The detected products varied linearly with laser power confirming the single photon nature of the process. The cross section of azomethane at 351 nm is ~1.9×10^{-20} cm^2, and with a photon flux of ~10^{18} photon/cm^2 per pulse, saturation of the initial photon absorption is highly unlikely.[2] Polarization measurements were performed using a "parallel plates polarizer" which consists of 10 quartz plates at Brewster's angle with respect to the direction of laser propagation. This resulted in >95% polarized light which could then be rotated by rotation of the polarizer.

Trans-azomethane was synthesized by the method of Renaud and Leitch[26] and was purified by trap to trap distillation prior to use.

III. Results and Discussion

Signal was collected at N_2^+ (m/e=28), CH_3^+ (m/e=15), CH_2^+ (m/e=14), and CH^+ (m/e=13) masses. The time dependent backgrounds due to dissociative ionization of the pulsed molecular beam were obtained by blocking the laser and were subtracted from the original signal. Time-of-flight spectra for CH^+ (m/e=13) and N_2^+ (m/e=28) at laboratory angles 20°, 35° and 50° are shown in Figures 2 and 3. Time dependent background from the beam pulse at m/e=15 (CH_3^+), the dominant daughter ion of azomethane, was sufficient to cause difficulty in subtraction. At m/e=14 (CH_2^+) there was significant contamination from N_2^{2+} or N^+. Since the first and second step methyl radicals should possess similar internal energies (within a few kcal/mole) they should exhibit comparable ionization cracking patterns. We therefore restrict ourselves to m/e=13, a daughter fragment of methyl radical, because of the superior signal-to-noise ratio. The data at m/e=13 fits well with a 1:1 ratio of first to second step methyls confirming the validity of this assumption. No detectable photodissociation signal was observed at the parent methyldiazenyl mass

(m/e=43) nor was there any indication of the presence of CH_3N_2 at the daughter masses suggesting that the CH_3N_2 fragment is short lived.

The two distinct peaks in Figure 2 correspond to a dissociation in which both methyl groups recoil with unequal velocities in the azomethane center-of-mass. Simultaneous *symmetric* fission of the identical C-N bonds would yield a single TOF peak reflecting the indistinguishability of the two methyl radicals. The data was initially fit by assuming that the two C-N bonds cleaved sequentially. Since there was ambiguity as to which peak in the methyl TOF spectra to assign to the initial impulse, two schemes, differing only in this assignment were considered. In both cases the dissociation was decomposed into two center-of-mass frames in which momentum is conserved.

A. Sequential Analysis

In the first sequential analysis it was assumed that the methyl that possesses a higher lab velocity originated from the initial dissociative impulse. The analysis was performed by using well known forward convolution techniques for treating the primary[27] and secondary dissociations[28] from photofragment translational spectroscopy experiments. The primary translational energy distribution, $P(E_T)$, shown in Figure 4a was derived from the fast component of the time-of-flight spectra of CH_3 shown in Figure 2 and assuming CH_3N_2 to be the other product. The distribution has an average value of 19.15 kcal/mole and a FWHM of ~10 kcal/mole. Since the CH_3N_2 fragment does not survive to the detector, it is not possible to "momentum match" the initial CH_3 as a means of gauging the integrity of the primary $P(E_T)$. However, by fitting the m/e=13 TOF over a wide range of laboratory angles, we have reasonable confidence in the derived primary $P(E_T)$. There was no observed correlation between the angle of laser polarization and the product intensity or

TOF profile. This corresponds to an anisotropy parameter of $\beta=0$[29] and indicates that the lifetime of the excited azomethane may be longer than its rotational period.

The slower peak in the m/e=13 time-of-flight spectra was then assigned as the second step methyl radical. If the CH_3N_2 intermediate persists for longer than its rotational period the secondary methyl radical should exhibit a bimodal velocity distribution reflecting forward-backward symmetry[30,31] in the secondary angular distribution $T(\theta)$ in the CH_3N_2 reference frame. The manifestation of only the slower component in the TOF spectra indicates that the second methyl radical is preferentially *backwards* scattered with respect to the CH_3N_2 recoil velocity vector. The secondary $P(E_T)$ derived from the TOF spectra is shown in Figure 4a.

The anomalously fast and narrow m/e=28 (N_2^+) time-of-flight spectra (Figure 3) are further evidence of an asymmetric angular distribution in the second step. The conservation of momentum requires that, for a methyl/nitrogen pair with a common CH_3N_2 parent, backward scattered CH_3 results in *forward* scattered N_2. Figure 5a shows a contour map illustrating the angular and velocity distributions of the photofragments in the CH_3N_2 center-of-mass. The arrows on the contour plot represent the most probable velocities that conserve momentum in the azomethane center-of-mass. The velocity vector at 0° is the CH_3 from the initial impulse. Although the angles appear to conflict with the peaks in the secondary angular distributions, the strong forward and backward peaks in $T(\theta)$ may be the result of two overlapping shoulders of sideways peaked distributions along the relative velocity vector of the initial dissociation step.

The data can also be analyzed, in a similar manner, by assuming that the *slow* methyl in the m/e=13 TOF spectra originates from the initial dissociation.

The $P(E_T)$ for this step is shown in Figure 4b. The distribution is peaked at 4 kcal/mole with a long high energy tail. A very impulsive translational energy release was required in the secondary dissociation in order to fit the fast component in the m/e=13 TOF spectra. The $P(E_T)$ for the secondary process is also shown in Figure 4b and is peaked significantly away from zero (~22 kcal/mole) with a FWHM of 12 kcal/mole. Not suprisingly, the strong angular correlation between the asymptotic velocities of all three photofragments, found in the preceding scheme, is also manifest in this method of analysis. Satisfactory fitting of the fast m/e=13 peak and the m/e=28 TOF spectra required that the nitrogen be scattered slightly forward and the methyl radical scattered backwards with respect to the CH_3N_2 velocity vector. Figure 5b shows the product of both the velocity and the most pronounced angular distribution for the secondary fragments in the CH_3N_2 center-of-mass.

B. CH_3N_2 Lifetime

The anisotropy in the secondary angular distributions implies a methyldiazenyl radical lifetime less that its rotation period. Secondary dissociation that proceeds before rotation of the primary photofragment indicates that the time interval between primary and secondary events is extremely short. The near simultaneous dissociation of two bonds is an accepted criterion for concertedness.[32] A tentative upper limit to the lifetime of the CH_3N_2 fragment can be estimated by first calculating the degree of rotational angular momentum generated from the initial impulse and then using the rotational period as a *clock* of the secondary process. Using the *cis* equilibrium geometry as a reasonable dissociative structure and assuming that the CH_3N_2 is rigid, the exit impact parameter, b, and hence the orbital (and rotational) angular momentum can be calculated by the following expression,

$$L=\mu bv=-J \quad (2)$$

where μ is the reduced mass of the two fragments and v is the relative velocity. The relative velocities of the initial fragments can be derived from the primary translational energy distributions and yield rotational periods of ~0.6 and ~1.5 ps suggesting that the lifetime is less than a picosecond. Our experiments clearly indicate that after the initial S_1<-S_0 excitation the excited molecules persist for many rotational periods. However, when the molecule starts to dissociate the two C-N bonds break almost simultaneously. Although there is some uncertainty in our result, there is certainly a large disparity between this lifetime and the one determined in previous experiments.[33] In light of the apparent brevity of the CH_3N_2 intermediate, the influence of collisions on vibrational relaxation of the primary CH_3N_2 product would appear to be unimportant even at moderate pressures. It is important to note that if the first step is not prompt, therefore providing no well defined time zero by which to clock the reaction, conventional time-resolved experiments are not feasible for studying the secondary processes of such systems.

C. Three Body Analysis

Based on the conclusions of the previous two sections, that the dissociation involves the asymmetric concerted rupture of both C-N bonds, it is prudent to analyze the data in terms of a three body dissociation rather than using a sequential scheme. The translational energy distributions for all three fragments in the azomethane center-of-mass, shown in Figure 6, were obtained by independent iterative fitting of each individual peak in the TOF spectra. Substantial translational energy was determined for the N_2 and one methyl

radical. The other CH_3 fragment has a $P(E_T)$ that is peaked close to zero with an average energy of ~4 kcal/mole. Since the two features in the methyl TOF spectra are not completely resolved, some uncertainty arises regarding the low energy tail of the fast methyl and the high energy portion of the slower methyl.

If the dissociation is concerted then of interest is the fraction of the *total* available energy partitioned into translation of all three fragments. The pertinent energetics for the near ultraviolet photodissociation of azomethane are shown in Figure 8. Absorption of a single 351 nm photon deposits 81.5 kcal/mole into azomethane. From the heats of formation for azomethane[34] (35.6 kcal/mole) and methyl radical[35] (35.0 kcal/mole) there should be 47.1 kcal/mole of available energy for the separation of all three fragments. The combined rotational and vibrational energy of azomethane at room temperature is estimated to be ~1.7 kcal/mole[17] and should be significantly reduced following the supersonic expansion. An average overall translational energy can be obtained from the mean translational energy of all three fragments. The average value of 28.2 kcal/mole corresponds to ~59.6% of the total available energy appearing as recoil of the photofragments.

The center-of-mass velocity distribution for each fragment was obtained directly from the calculated $P(E_T)$ and used in the generation of the vector diagram shown in Figure 7. The nitrogen has a most probable center-of-mass velocity of 2180 m/s and methyl radicals recoil with mean velocities of 3300 m/s and 1350 m/s. Conservation of linear momentum determines the angles between all three fragments given the most probable center-of-mass velocity of each fragment. The asymptotic angle between N_2 and the faster CH_3 is approximately 160° as would be expected, intuitively, if these two fragments experienced the majority of the repulsive energy released during the

dissociation. The derived vector relations of the three fragments is in good agreement with those derived from the sequential analysis.

D. Dissociation Mechanism

Any proposed mechanism of azomethane dissociation must be consistent with both the angular correlation of the photofragments and the unequal partitioning of translational energy between the two departing methyl radicals. A mechanism in which simultaneous asymmetric scission of the C-N bonds is driven by the pairing of electrons to form the N-N triple bond fulfills the above requirements. This is feasible because the CH_3N_2 intermediate is *unstable* with respect to elimination of CH_3.[36] The extension of one C-N bond, therefore, need only to reach a critical length in azomethane where electronic rearrangement and synchronous C-N bond cleavage can occur. The CH_3 group that is farthest removed from the CH_3N_2 as the closed shell N_2 is formed behaves much like a "spectator" during the dissociation and receives only a modest degree of recoil. However, the other CH_3, due to its proximity to the N_2, experiences the majority of the repulsive potential energy release. This mechanism is similar to the elimination of molecular hydrogen from ethylene[37] and formaldehyde.[38,39] In both cases one C-H bond elongates considerably more than the other, and as the H_2 molecule forms, the impulses along the C-H bonds are unequal resulting in considerable rotational excitation of the H_2. If this is indeed the mechanism of dissociation, it may be important in understanding similar systems that undergo molecular elimination concurrent with the formation of further unsaturation. For example, following the loss of one iodine atom from CH_2ICH_2I, the loss of the second iodine and formation of ethylene is exothermic.[40] The dissociation of the two C-I bonds may also occur, therefore, simultaneously when one C-I bond reaches a critical distance.

The lack of observable fluorescence from the S_1 state indicates that azomethane may undergo either internal conversion (IC) or intersystem crossing (ISC) rapidly. Furthermore, the lack of correlation between the angle of laser polarization and the measured product angular distributions suggest that the dissociation may not be from the S_1 state initially populated. Although the first triplet state, T_1, lies below S_1 in energy there has been conflicting evidence for its relevance. No phosphorescence has ever been observed from any azoalkane necessitating the use of indirect means to study the potential participation of T_1.[1,11] Triplet sensitized reactions have been effective in achieving azomethane decomposition but exhibit much lower quantum yields for dissociation than photolysis.[1] It has been debated whether or not this is due to an alternate mechanism that does not proceed via the triplet state, the involvement of a *second* triplet surface, or the efficiency of energy transfer from the sensitizer to the azoalkane. The last argument would support the existence of a *barrier* on the triplet surface. If sufficient energy is not deposited into the triplet state to overcome the barrier to dissociation deexcitation competes effectively with decomposition. Certainly our results are consistent with this mechanism. Intersystem crossing followed by dissociation over a barrier on the triplet potential energy surface would account for both the finite excited state lifetime and impulsive energy release observed. The transition state on the excited triplet potential energy surface is predicted, by *ab initio* calculation[19], to be asymmetric with one C-N bond 34% longer than the other which remains close to its equilibrium bond length.

If internal conversion occurs readily in the *gas phase* then the dissociation could proceed from the ground state potential energy surface. Internal conversion in azomethane has been predicted to be facilitated by the proximity of the S_1 and S_0 states in both the twist and semilinear geometries.[7] This allows

IC to occur without the participation of the excited triplet state. Significant rotation about the N-N bond on the S_1 state prior to IC will insure that both ground state cis and trans isomers would be equally populated. The thermal barrier to isomerization is thought to be ~50 kcal/mole[7,41] so that further isomerization may take place on the ground state surface depending on the relative rate of isomerization compared to dissociation. Although the relative energies of cis and trans azomethane have not been experimentally observed, the cis isomer has been estimated to be several kcal/mole higher in energy.[7] The large amplitude motion that is expected based on the quantity of internal energy would certainly allow reaching a highly asymmetric configuration on the ground state potential energy surface. In spite of RRKM calculations[42] in conjunction with time-resolved work[16], which find that a ground state dissociation is highly improbable, the results of this experiment show no evidence to suggest that the dissociation could not occur from the S_0 state.

IV. Concluding Remarks

Azomethane has been shown by photofragment translational spectroscopy to undergo dissociation to two methyl radicals and nitrogen following excitation to its first excited singlet state. We find that there is a strong correlation of the asymptotic velocity vectors of all three fragments indicating that the dissociation is concerted rather than stepwise as had been previously reported. The overall translational energy distributions for all three fragments in the azomethane center-of-mass clearly illustrate the disparate partitioning of energy between the two recoiling methyl fragments. If the dissociation occurs via a transition state that is asymmetric with regards to the C-N bond lengths, then a simultaneous pairing of the electrons to form the N-N triple bond would result in the departing CH_3 groups having vastly different recoil velocities. The

electronic state from which the dissociation proceeds, however, remains unclear.

The utility of this technique to clearly differentiate between concerted and stepwise mechanisms is impressive. It is also important to note that since non-adiabatic transitions may occur prior to dissociation, the excited azomethane will possess a finite lifetime. However, since once dissociation commences, both C-N bonds cleave in rapid succession conventional pump and probe time-resolved experiments are not feasible for studying the relation between the first and second bond ruptures in such a system. Further experiments using infrared multiphoton dissociation (IRMPD) in a molecular beam should provide valuable insight into the ground state decomposition of azomethane and increase our understanding of its ultraviolet photochemistry.

Acknowledgements. The authors would like to thank Jim Meyers for improvements to the CMLAB data analysis program. SWN wishes to acknowledge R.B. Weisman for many helpful discussions. This work was supported by the Director, Office of Energy Research, Office of Basic Energy Sciences, Chemical Sciences Division of the U.S. Department of Energy under contract No. DE-ACO3-76SF00098.

Registry No. azomethane, 503-28-6; methyl, 2229-07-4; nitrogen, 7727-37-9.

References and Notes:

1. Engel, P.S., *Chem. Rev.*, **80**(2), (1980); Engel, P.S., Steel, C., *Acc. Chem. Res.*, **6**, 275, (1973); Calvert, J.G., Pitts, J.N., Photochemistry, (Wiley, New York, 1966).
2. Collier, S.S., Slater, D.H., Calvert, J.G., *Photochem. Photobiol.*, **7**, 737, (1968); M.B. Robin, B.R. Hart, N.A. Kuebler, *J. Am. Chem. Soc.*, **89**(7), 1564, (1967); Mosher, O.A., Foster, M.S., Flicker, W.M., Beauchamp, J.L., Kuppermann, A., *J. Chem. Phys.*, **62**(9), 3429, (1975).
3. Cannon, C.V., Rice, O.K., *J. Am. Chem. Soc.*, **63**, 2900, (1941); Jones, M.H., Steacie, E.W.R., *J. Chem. Phys.*, **21**, 1018, (1953).
4. Macpherson, M.T., Pilling, M.J., Smith, M.J.C., *Chem. Phys. Lett.*, **94**, 430, (1983); Braggott, J.E., Brouard, M., Coles, M.A., Davis, A, Lightfoot, Macpherson, M.T., Pilling, M.J., *J. Phys. Chem.*, **91**, 317, (1987).
5. G. Herzberg, *Proc. Roy. Soc.*, A **262**, 291 (1961); T.G. DiGiuseppe, J.W. Hudgens, M.C. Lin, *J. Phys. Chem.*, **86**, 36, (1982).
6. Chu, P.M., Ph.D. Thesis, University of California, Berkeley, 1991; North, S.W., Chu, P., Lee, Y.T., unpublished results.
7. Camp, R.N., Epstein, I.R., Steel, C., *J. Am. Chem. Soc.*, **99**(8), 2453, (1977).
8. Although the second triplet state is thought to be energetically inaccessible at ~360 nm there is some evidence that T_2 lies below S_1 in energy and may be important in the photochemistry; see for example Baird, N.C., Swenson, J.R., *Can. J. Chem.*, **51**, 3097, (1973); *ref 7*.
9. Rapid for S_1->T_2 intersystem crossing.
10. Engel, P.S., *J. Am. Chem. Soc.*, **91**, 6903, (1969).
11. Durr, H., Rege, B., *Top. Curr. Chem.*, **66**, 53, (1976) and references therein.
12. Dewar, M.J.S., *J. Am. Chem. Soc.*, **106**, 209, (1984).
13. Donaldson, D.J., Leone, S.R., *J. Chem. Phys.*, **85**, 877, (1986).
14. Trentelman, K.A., Kable, S.H., Moss, D.B., Houston, P.L., *J. Chem. Phys.*, **91**(12),

7498, (1989).

15. Holt, P.L., McCurdy, K.E., Adams, J.S., Burton, K.A., Weisman, R.B., Engel, P.S., *J. Am. Chem. Soc.*, **107**, 2180, (1985).

16. Burton, K.A., Weisman, R.B., *J. Am. Chem. Soc.*, **112**, 1804, (1990).

17. Andrews, B.K., Burton, K.A., Weisman, R.B., *J. Chem. Phys.*, **96**(2), 1111, (1992).

18. Takagi, K., Crawford, R.J., *J. Am. Chem. Soc.*, **93**, 5910, (1971); Mendenhall, G.D., Chen, T.E., *J. Phys. Chem.*, **84**, 2849, (1985).

19. Andrews, B.K., Weisman, R.B., unpublished results.

20. Dannenberg, J.J., *J. Org. Chem.*, **50**, 4963, (1985).

21. Yamashita, K., Kaminoyama, M., Yamabe, T., Fukui, K., *Chem. Phys. Lett.*, **83**, 78, (1981).

22. Weisman, R.B., personal communication.

23. Lee, Y.T., McDonald, J.D., LeBreton, P.R., Herschbach, D.R., *Rev. Sci. Instrum.*, **40**, 1402, (1969).

24. Proch, D., Trickl, T., *Rev. Sci. Instrum.*, **60**, 713, (1989).

25. see for example; Felder, P., Effenhauser, C.S., Haas, B.M., Huber, J.R., *Chem. Phys. Lett.*, **148**(5), 417, (1988).

26. Renaud, R., Leitch, L.C., *Can. J. Chem.*, **32**, 545, (1954).

27. Wodtke, A.M., Ph.D. Thesis, University of California, Berkeley, 1986; Zhao, X., Ph.D. Thesis, University of California, Berkeley, 1988.

28. Zhao, X., Nathanson, G.M., Lee, Y.T., *Acta Physico-Chimica Sinica*, **8**(1), (1992).

29. Zare, R.N., Ph.D., Harvard University, 1964; Zare, R.N., *Mol. Photochem.*, **4**,1, (1972).

30. Miller, W.B., Safron, S.A., Herschbach, D.R., *Chem. Soc., Faraday Disc.*, **44**, 108, 292 (1967); *J. Chem. Phys.*, **56**, 3581 (1972).

31. Kroger, P.M., Riley, S.J., *J. Chem. Phys.*, **67**, 4483, (1977); Kroger, P.M., Riley, S.J., *J. Chem. Phys.*, **70**, 3863, (1979); Hintsa, E.J., Zhao, X., Lee, Y.T., *J. Chem. Phys.*, **92**, 2280, (1990).

32. Strauss, C.E.M., Houston, P.L., *J. Phys. Chem.*, **94**, 8751, (1990).

33. Photodissociation of azomethane at 355 nm in our laboratory has confirmed that the ~1 kcal/mole difference in excitation energy between the two experiments has an insignificant effect upon the observed dynamics.

34. Engel, P.S., Montgomery, R.L., Mansson, M., Leckonby, R.A., Foyt, H.C., Rossini, F.D., *J. Chem. Thermodyn.*, **10**, 205, (1978).

35. Benson, S.W., Thermochemical Kinetics, 2nd ed., (Wiley, New York, 1976).

36. Engel, P.S., Wood, J.L., Sweet, J.A., Margrave, J.L., *J. Am. Chem. Soc.*, **96**, 2381, (1974); Acs, G., Peter, A, *Int. J. Chem. Kinet.*, **19**, 929, (1981).

37. Balko, B.A., Zhang, J., Lee, Y.T., *J. Chem. Phys.*, **97**(2), 935, (1992); Stolow, A., Balko, B.A., Cromwell, E.F., Zhang, J., Lee, Y.T., *J. Photochem. Photobiol.*, (1992); Cromwell, E.F., Stolow, A., Vrakking, M.J.J., Lee, Y.T., *J. Chem . Phys.*, **97**, 4029, (1992).

38. Goddard, J.D., Schaefer, H.F., *J. Chem. Phys.*, **70**, 5117, (1979).

39. Houston, P.L., Moore, C.B., *J. Chem. Phys.*, **65**, 757, (1976).

40. Benson, S.W., Amano, A., J. Chem. Phys., **36**, 3464, (1962); *JANAF Thermochemical Tables*, 2nd ed., Natl. Stand. Ref. Data Sr. U.S. Natl. Bur. Stand. 37 (U.S. GPO, Washington, D.C., 1971).

41. Acs, G., Peter, A., *Int. J. Chem. Kinetics*, **19**, 929, (1987).

42. Andrews, Burton, B.K., Weisman, R.B., unpublished results.

FIGURE CAPTIONS

Figure 1 The schematic diagram of the fixed source rotatable detector apparatus. (1) pulsed valve (2) cryopanel cooled to ~6K (3) interaction region of the laser and the molecular beam (4) electron bombardment ionizer (5) quadrupole mass filter.

Figure 2 Time-of-flight spectra for m/e=13 (CH^+) at laboratory angles 20°, 35° and 50°.The open circles represent data points. The contributions from the first (····) and second (—) step methyl radicals as well as the total fit are the forward convolutions of both the primary and secondary center-of-mass translational energy distributions shown in Figure 4b and T(θ) shown in Figure 5b.

Figure 3 Time-of-flight spectra for m/e=28 (N_2^+) at laboratory angles 20°, 35°, and 50°. The slow signal in the spectrum at 20° is due to time dependent background from the pulse valve. The fit is the forward convolution of the two translational energy distributions shown in Figure 4b and T(θ) shown in Figure 5b.

Figure 4 The primary (—) and secondary (·····) translational energy distributions derived from the two sequential analyses (see text).

Figure 5 Contour plots of the secondary velocity distributions for CH_3 (—) and N_2 (·····). Each plot corresponds to a sequential analysis described in the text. Arrows show the primary impulse (0°) and the most probable secondary velocities that conserve momentum.

Figure 6 The translational energy distributions for each fragment in the azomethane center-of-mass.

Figure 7 Newton diagram in the azomethane center-of-mass showing the most probable velocities of all three fragments in solid lines.

Figure 8 Energy level diagram for the 351 nm photodissociation of azomethane.

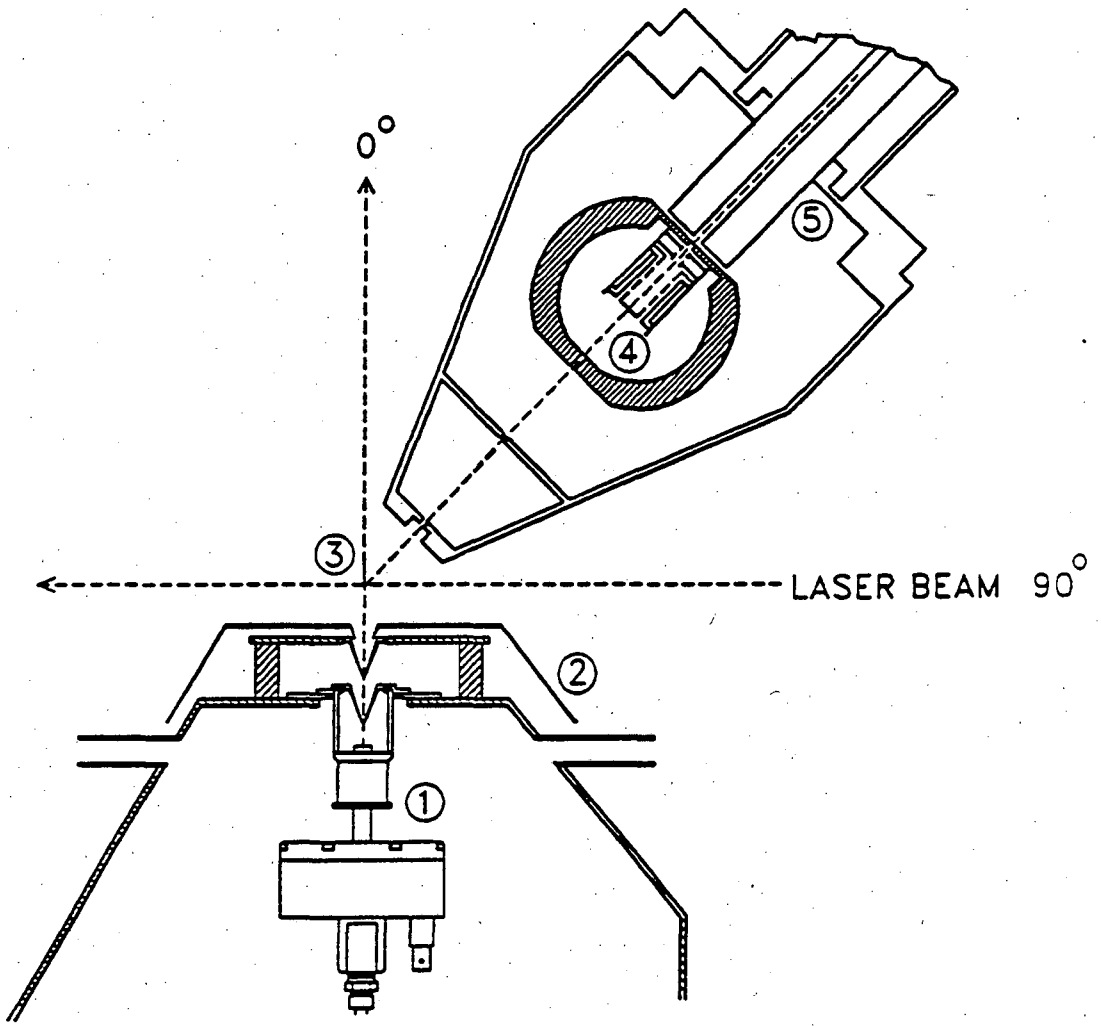

Figure 1.

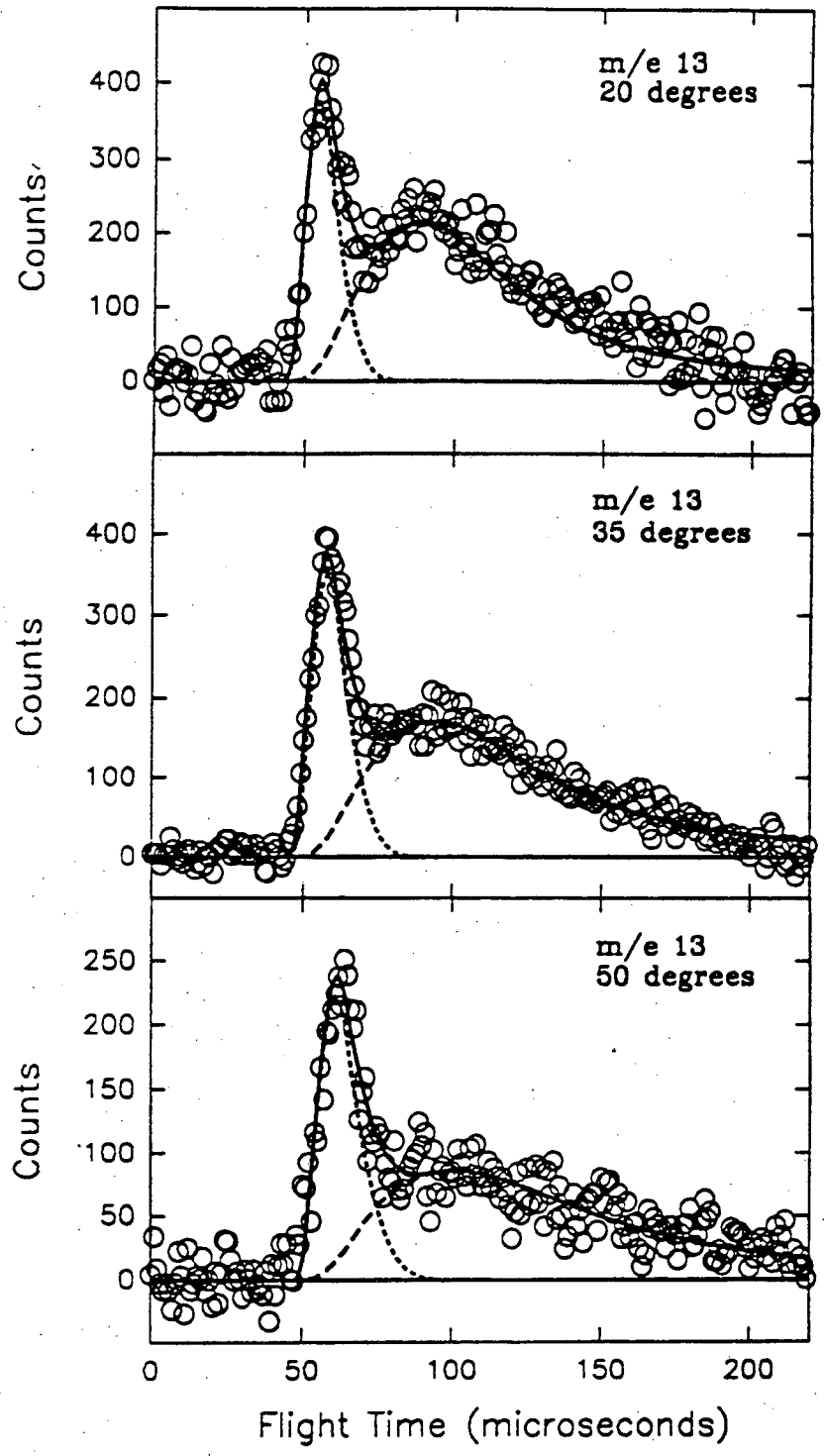
m/e 13
20 degrees
m/e 13
35 degrees
m/e 13
50 degrees
Counts
Counts
Counts
400
300
200
100
0
400
300
200
100
0
250
200
150
100
50
0
0
50
100
150
200
Flight Time (microseconds)

Figure 2.

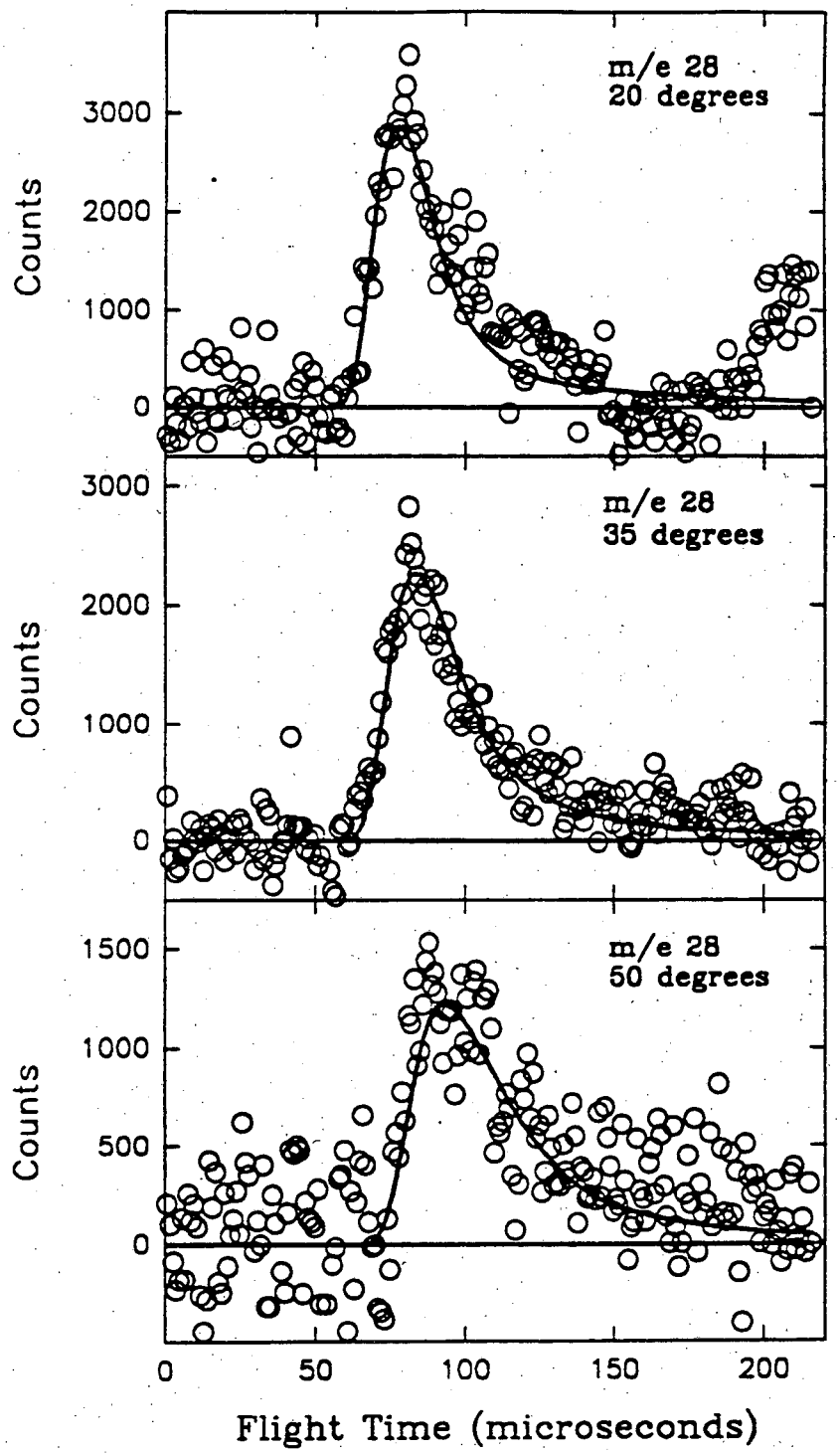
m/e 28
20 degrees
m/e 28
35 degrees
m/e 28
50 degrees
Counts
3000
2000
1000
0
1500
500
0
50
100
150
200
Flight Time (microseconds)

Figure 3

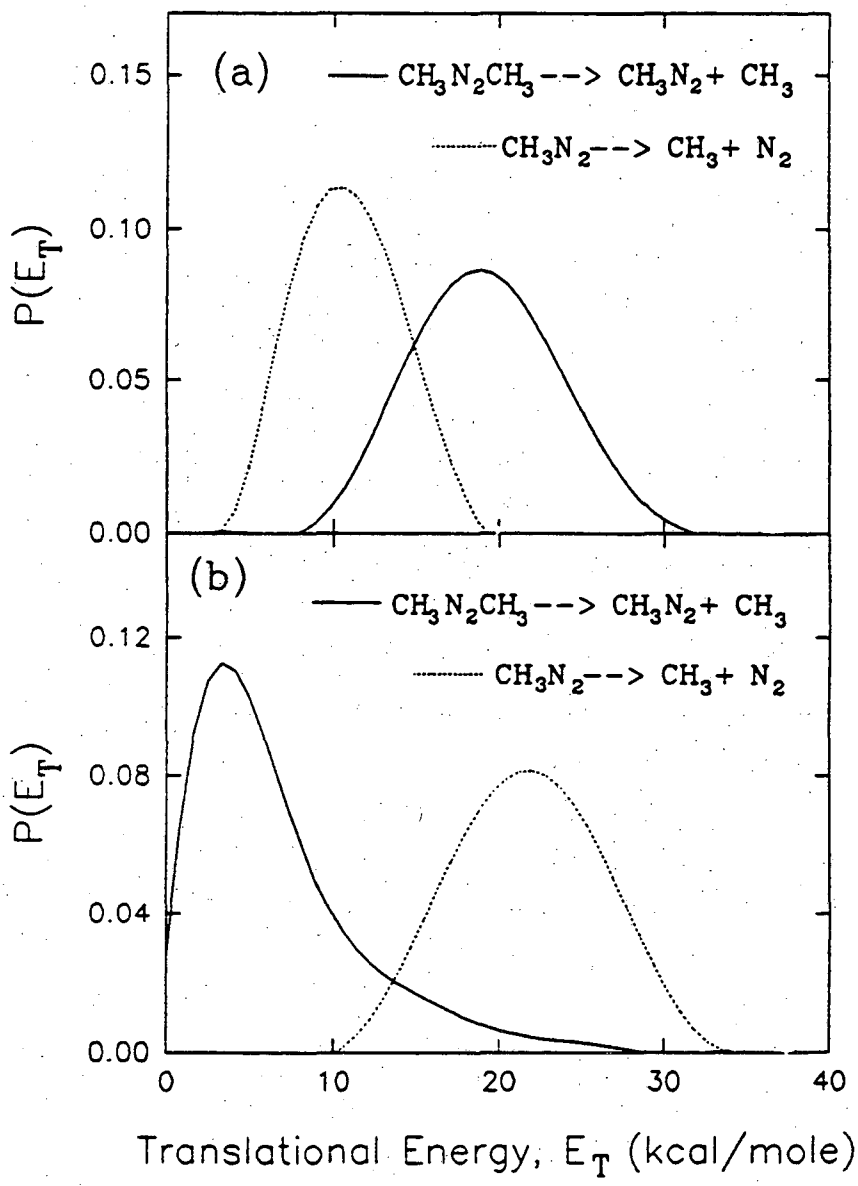
(a)
CH3N2CH3--> CH3N2+ CH3
CH3N2--> CH3+ N2
0.15
0.10
0.05
0.00
P(ET)
(b)
CH3N2CH3--> CH3N2+ CH3
CH3N2--> CH3+ N2
0.12
0.08
0.04
0.00
P(ET)
0
10
20
30
40
Translational Energy, ET (kcal/mole)

Figure 4.

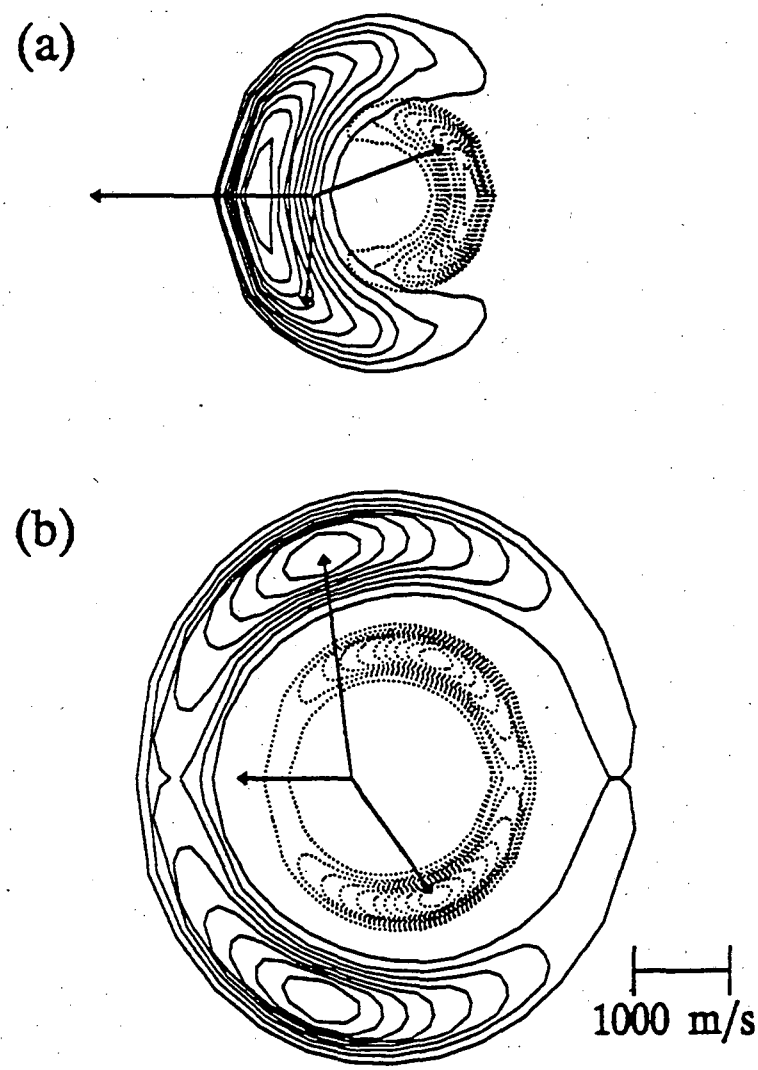

Figure 5.

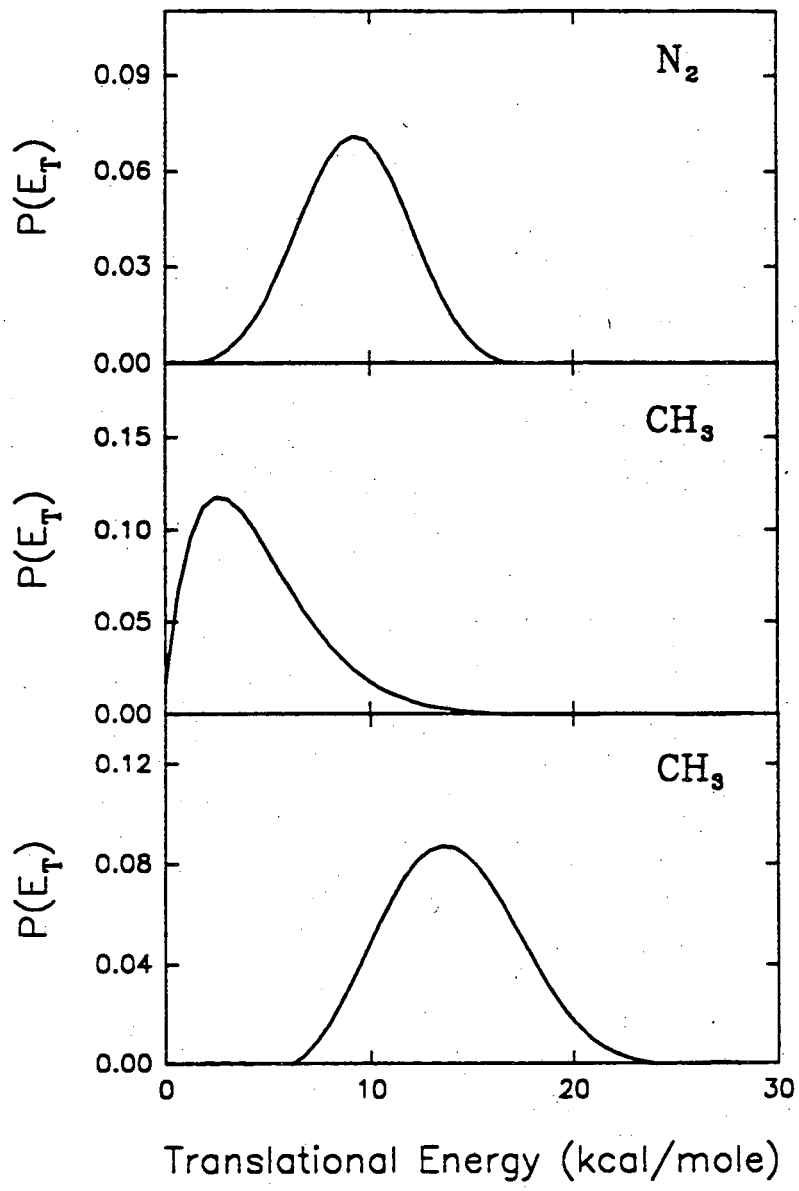
N2
CH3
CH3
P(ET)
P(ET)
P(ET)
0.09
0.06
0.03
0.00
0.15
0.10
0.05
0.00
0.12
0.08
0.04
0.00
0
10
20
30
Translational Energy (kcal/mole)

Figure 6.

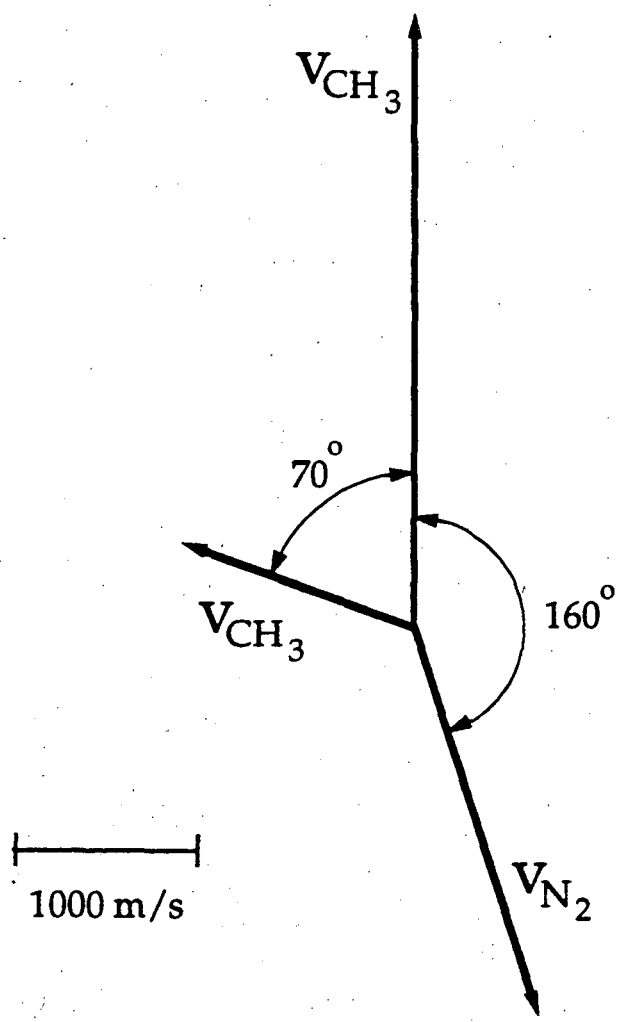

Figure 7.

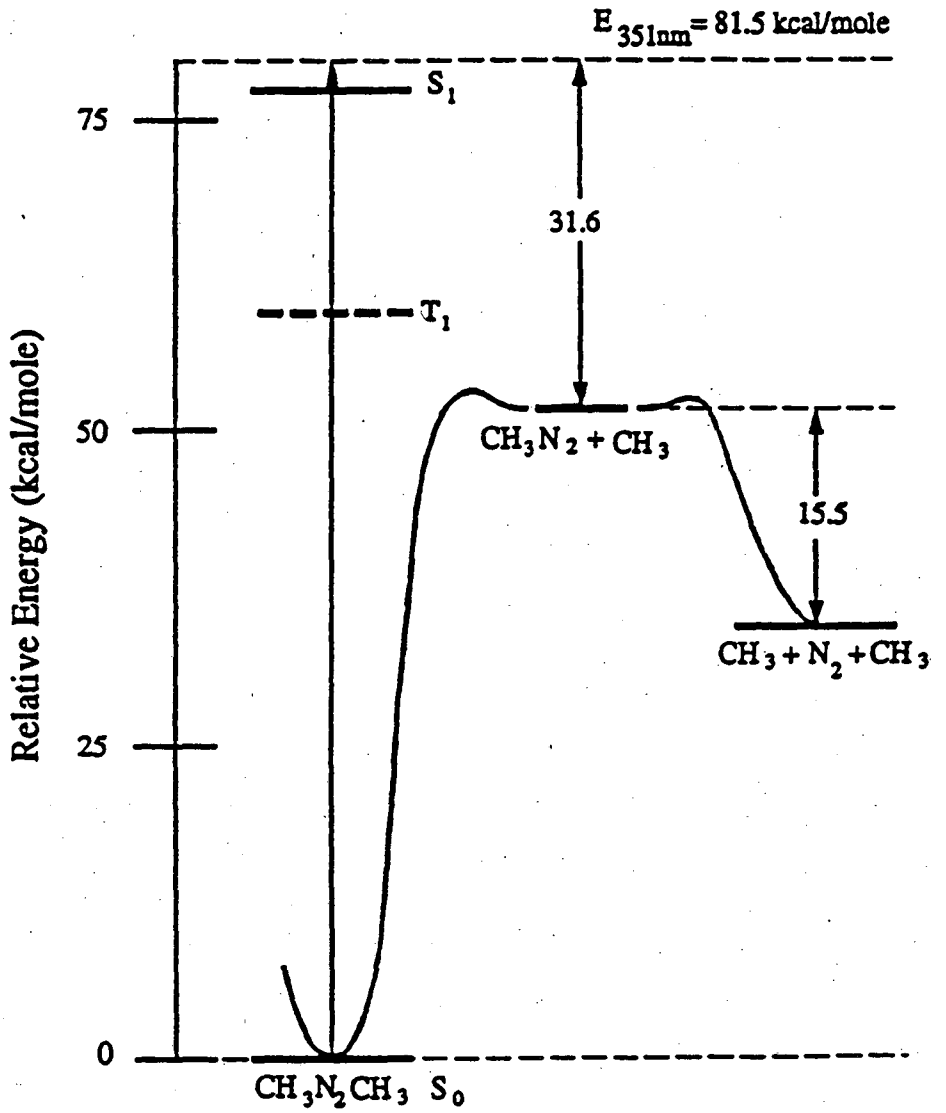
E 351nm = 81.5 kcal/mole
S1
T1
75
50
25
0
31.6
15.5
CH3N2 + CH3
CH3 + N2 + CH3
CH3N2CH3 S0
Relative Energy (kcal/mole)

Figure 8.

LAWRENCE BERKELEY LABORATORY
UNIVERSITY OF CALIFORNIA
TECHNICAL INFORMATION DEPARTMENT
BERKELEY, CALIFORNIA 94720